Convex Surface Heat Transfer Behaviour in the Presence of Obliquely Impinging Non-Isothermal Slot Jets

Satyanand Abraham, Abhijeet B. Kakade and R. P. Vedula

***Abstract*—Experimental measurements for the circumferential variation of Nusselt number and effectiveness for a straight and an inclined slot jet impinging on a convex cylindrical surface are reported in this study. The curvature ratio defined as the ratio of slot width to diameter of impingement target surface (b/D) was kept constant at 0.045. Data are reported for Reynolds numbers, based on the velocity of the jet and width of the slot, equal to 5500 and 8500 for jets inclined at 0^0, 30^0 and 45^0 to the jet axis. The non dimensional distances between jet exit and apex of the convex surface (H/b) equal to 4, 6, 8 and 10 were studied. The results show that with obliquely impinging jets the maximum Nu shifts towards the uphill side. The effectiveness distribution is affected more significantly than the heat transfer distribution. The variation of effectiveness decreases on the downhill side but exhibits a rapidly decreasing trend on the uphill side with increase in inclination angle.**

Keywords: Convex surface, Effectiveness, heat transfer, inclined slot jet, impingement

I. Introduction

JET impingement heat transfer is characterized by high localized heat transfer coefficients which are useful in the cooling of surfaces which experience severe thermal environments. This technique is widely used in food, textile, paper industries and gas turbines for cooling and heating process. An impinging jet with a temperature equal to the surrounding ambient is typically referred to as an isothermal jet while a jet which is different in temperature from the surrounding ambient is referred to as a non-isothermal jet. An isothermal jet requires the heat transfer coefficient as the only parameter to characterize the heat transfer performance, whereas a non isothermal jet requires an additional parameter, effectiveness, which characterizes the entrainment of the surrounding fluid by the impinging jet.

Heat transfer results for an isothermal slot jet impinging on a cylindrical convex surface for various relative curvatures, ratio of jet diameter to diameter of curved surface, b/D, were presented in [1]. At higher circumferential distance values, surfaces with lower curvature were reported to experience higher Nu, Nusselt number based on slot width. This was attributed to the flow stabilizing behavior of curvature and the resulting reduction in momentum and energy transport. Heat transfer results for a circular jet impinging on a hemispherical convex surface were reported in [2]. The maximum stagnation Nu was observed at H/d=6 for lower Reynolds numbers and increased to 8 for higher Reynolds numbers. The stagnation Nu was reported to increase with increasing relative curvature. The Nusselt number distribution along the circumferential direction was reported to be relatively insensitive to curvature ratio after r/d=2. A secondary maximum at r/d=2 was also reported. Heat transfer data for a circular jet impinging obliquely on hemispherical convex surface was reported in [3]. Results show a shift in the maximum Nusselt number from the geometric stagnation point to a maximum of 0.67 times the nozzle diameter towards the uphill side.

Experimental data for effectiveness of a circular non-isothermal jet impinging on a flat plate were presented in [4]. The effectiveness was reported to be independent of Reynolds number and decrease with increasing H/d. The drop was reported to be very significant for values of distance between the plate and jet greater than the length of the potential core. Analytical calculations of effectiveness were presented in [5] and the match with experimental data for H/d>5 and x/d>2 was reported to be satisfactory.

There is a reasonably large volume of work reported for the heat transfer performance of isothermal jets impinging on a convex surface. However, studies for non-isothermal jets are not available either for normal or inclined impinging slot jets. The present study reports the heat transfer coefficient and effectiveness distribution for normal and inclined non-isothermal jets impinging on a cylindrical convex surface.

II. Experimental Setup and Methodologies

A schematic of the experimental setup used in the current study is shown in Fig. 1. Air supplied by a compressor was first stored in a pressure vessel and then routed through a control valve and venturi meter to a plenum chamber. The pressure drop across the venturi meter measured by a water manometer was used to calculate the volume flow rate. The absolute pressure measured at the throat of the venturi meter was used to estimate the density to calculate the mass flow rate from the measured volume flow rate. Provision for heating the jet to a temperature well above ambient was included by providing two heaters in series in the flow path

Manuscript received March 05, 2015; revised March 26, 2015.

S. Abraham is with Indian Institute of Technology, Bombay, India (Ph: +919820727846; e-mail: satyanand.abraham@yahoo.com).

A.B. Kakade is with Indian Institute of Technology, Bombay, India (e-mail: abkakadenec@gmail.com).

R. P. Vedula is with Indian Institute of Technology, Bombay, India (e-mail: rpv@iitb.ac.in).

ISBN: 978-988-14047-0-1
ISSN: 2078-0958 (Print); ISSN: 2078-0966 (Online)

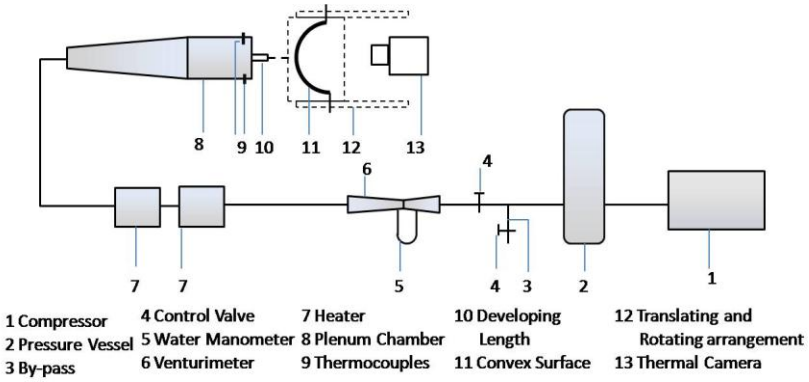

Fig. 1 Schematic of experimental setup

after the venturi meter. Air from the heaters was passed into the plenum chamber which had an initial diverging angle of 10° and then subsequently a constant area duct to accomplish uniform flow at the exit section to which the jet plate was connected. The jet plate had an accurately machined slot to which a rectangular section was connected which provided developing length equal to ten slot width before the jet emerged. The heaters and the setup downstream of heaters were insulated to minimize heat loss to the ambient. The jet temperature was measured with 8 thermocouples at the exit of the plenum chamber.

The slot jet height to width ratio was kept constant at 40. A stainless steel foil of thickness 0.11 mm was used for making the cylindrical convex impingement plate whose diameter was chosen such that the curvature ratio (b/D) was equal to 0.045. The impingement plate was attached to a traversing mechanism which was used to change H/b and inclination with respect to the jet. The ratio of the impinging surface distance from the jet to the jet width, H/b, was varied between 4 and 10. To study heat transfer and effectiveness of inclined impinging jets, the target plate was inclined instead of inclining the jet as shown in Fig. 2. The inclination was measured from jet axis with $\theta=0^0$ being the configuration perpendicular to convex surface. Two Reynolds numbers, based on jet exit velocity and width of slot, equal to 5500 and 8500 were studied for 0^0, 35^0 and 45^0 inclination angles.

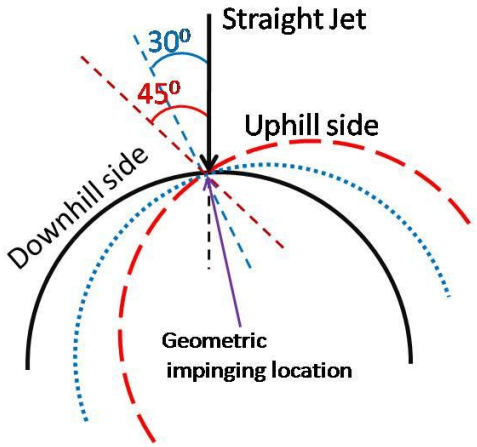

Fig. 2 Inclination of curved plate

The inclination was provided in such a manner that the centre of the plate was always the geometric impingement point. The inclined jet can also be viewed as a normal jet with the geometric impingement point linearly offset from the 0^0 inclination configuration since the impingement surface is a cylindrical one.

Copper bus bars soldered to the ends of the impinging surface were connected to an AC power source and current was passed through the curved surface to heat it. The jet impinged on the convex surface and the concave side of the impingement plate was painted black and a thermal image of the concave surface was taken with an infrared camera to obtain the wall temperature distribution under steady state

NOMENCLATURE

Symbol	Quantity	Unit in SI
$\mathbf{A_{foil}}$	Area of foil	m^2
b	Width of slot	m
D	Diameter of convex surface	m
H	Jet- to-plate distance	m
h	Heat transfer coefficient	W/m^2K
I	Current	A
$\mathbf{k_a}$	Thermal conductivity of air	W/mK
$\mathbf{k_s}$	Thermal conductivity of steel	W/mK
Nu	Nusselt number	hb/k_a
q	Heat transfer	W
q"	Heat flux	W/m^2
$\dot{q}$	Heat generation	W/m^3
Re	Reynolds number based on jet exit velocity and slot width	U_jb/v
r	Direction along convex surface	
T	Temperature	K
t	Thickness of steel foil	m
$\mathbf{U_j}$	Velocity of jet at exit	m/s
V	Voltage	V
	Subscripts	
amb	Ambient	
aw	Adiabatic	
b	bulk	
h	heated	
iso	isothermal	
j	Jet	
loss	loss	
w	Wall	
	Greek	
θ	Inclination of impinging surface with jet center line	
η	effectiveness	
ν	kinematic viscosity of air	

ISBN: 978-988-14047-0-1
ISSN: 2078-0958 (Print); ISSN: 2078-0966 (Online)

conditions. The thermal camera was calibrated with respect to a calibrated thermocouple that was embedded in an isothermal copper block which was coated with same black paint as used on the test section. The uncertainty in calibration was determined to be ± 1.2^0C with 99.5% confidence. The concave surface experienced a heat loss also since it was exposed to ambient. This heat loss was experimentally measured by insulating the convex surface and supplying heat to the surface such that it reached temperature values encountered in the experiments with impingement. The total heat input to the foil was evaluated as the product of voltage drop across the foil and the current flowing through it. The net heat flux transferred to the jet was calculated as the difference between the total heat flux given and the heat flux lost to surrounding as in eq. (1).

$$q_{total} = VI \qquad q_w^{"} = \frac{q_{total} - q_{loss}}{A_{foil}} \tag{1}$$

The temperature gradients near the stagnation point are large and to account for possible errors due to thermal conduction effects, a simple methodology suggested in [6] was used. Since the wall thickness is small, the temperature gradient was ignored in this direction.

The local heat transfer coefficient at a given location was calculated by considering neighboring temperatures also. An energy balance for the finite volumes shown in Fig. 3 was used to obtain the equation (2) for the heat transfer coefficient. Since experimental data had a small local scatter a smoothing curve was passed through the data when using this correction. The Nusselt number 'Nu' is calculated using the width of jet 'b' as characteristic length.

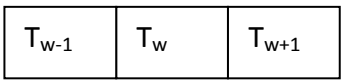

Fig. 3 Adjacent finite volumes

$$h_{iso} = \frac{\dot{q}t + k_s\left(\frac{T_{w-1} + T_{w+1} - 2T_w}{(dx)^2}\right)t - q''_{loss}}{(T_w - T_b)} \tag{2}$$

$$Nu = \frac{h_{iso}\ b}{k}$$

In non-isothermal experiments a hot jet was used which entrains the relatively cooler surrounding fluid. The effectiveness which is also required to evaluate the heat transfer performance is defined as follows.

$$\eta = \frac{T_{aw} - T_{amb}}{T_j - T_{amb}} \tag{3}$$

T_{aw} is the adiabatic wall temperature, i.e. temperature of the wall when no heat transfer happens from the wall. The method for calculating T_{aw} explained in [7] is as follows.

$$q_w^{"} = h_h(T_w - T_{aw}) = h_h T_w - h_h T_{aw} \tag{4}$$

Since h_h and T_{aw} are constants, the slope of plot of $q_w^{"}$ vs T_w at each location gives h_h at that location and the T_{aw} can be calculated from intercept on the temperature axis. Experiments were conducted with 4 different heat fluxes and it was found that $q_w^{"}$ vs T_w plots were always linear. A typical case with $\theta=0^0$, Re=8500 and H/b=4 is shown in Fig. 4

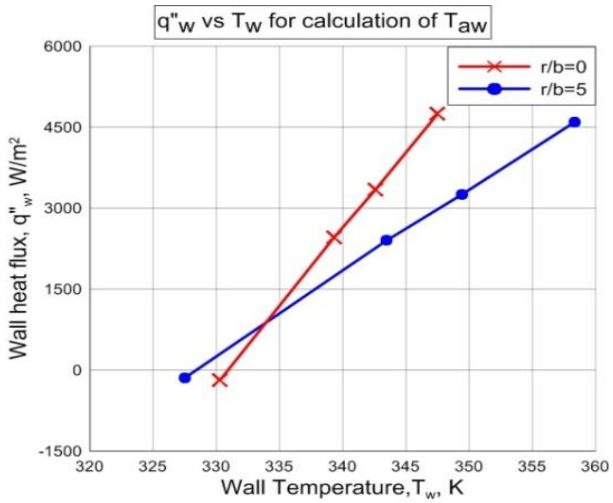

Fig. 4 $q"_w$ vs T_w for calculation of T_{aw}

The uncertainty in Nusselt number and effectiveness calculated using the methodology explained in [8] are 9.3% and 7.1% respectively.

III. RESULTS AND DISCUSSION

Results from experiments with slot jet impinging on convex surface at different angles of inclinations are presented here. Experiments were done both for isothermal and heated jets. The heated jet experiments provided data on effectiveness. Fig. 5 shows a comparison of the Nusselt number from present study with [1] and the data are found to be matching reasonably well providing confidence in the experimental methodologies adopted

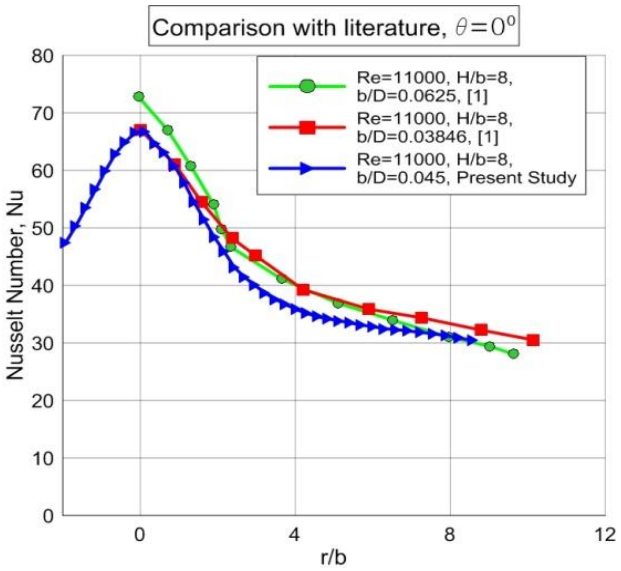

Fig. 5 Comparison of Nusselt number with literature for normal impinging jets

ISBN: 978-988-14047-0-1
ISSN: 2078-0958 (Print); ISSN: 2078-0966 (Online)

A. CYLINDRICAL CONVEX SURFACE WITH STRAIGHT IMPINGING JETS.

Fig. 6 and Fig. 7 show the circumferential variation of Nusselt number and effectiveness for Re=5500 and 8500 for 0^0 inclination angle for all jet-to-plate distances studied. The stagnation Nu increases as H/b increases till H/b=6 and 8 for Re=5500 and 8500 respectively and then falls.

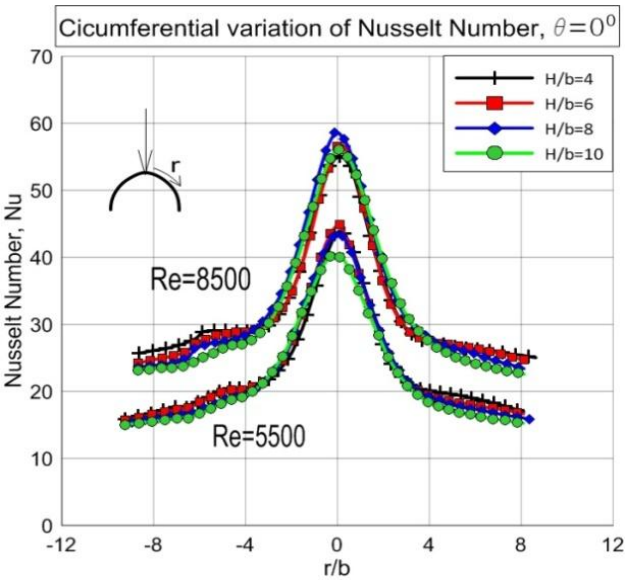

Fig. 6 Circumferential variation of Nusselt number for $\theta=0^0$

For all jet-to-plate distances, maximum effectiveness is observed at geometric stagnation point. The stagnation point effectiveness is near unity for the lowest H/b value and progressively reduces with increase in jet to impinging surface distance. The rate of reduction in effectiveness in the circumferential direction is higher for smaller H/b. The entrainment of ambient air by the incoming jet is less for lower H/b values before striking the surface resulting in high effectiveness values at the stagnation point. As the flow moves out in the circumferential direction more fluid gets entrained and effectiveness reduces. As H/b increases, the incoming jet entrains more fluid from the surrounding ambient before impingement thereby reducing the stagnation effectiveness value. At large values of r/b, the entrainment becomes so large that the differences between the different H/b values become small.

The variation of effectiveness with Reynolds number is presented in Fig. 8 and the effect is negligible. This lack of dependence of effectiveness on Reynolds number has also been reported for jet impinging on a flat surface in [4] and is attributed to the absence of the influence of Re on entrainment of the surrounding fluid by the jet.

B. CYLINDRICAL CONVEX SURFACE WITH OBLIQUELY IMPINGING JETS.

The circumferential variations of Nu for two inclinations, 35^0 and 45^0, and two Reynolds numbers for all H/b ratios studied are shown in

Fig. 9. The shift of the peak Nusselt number towards the uphill side is clearly observed. The shift is maximum for $\theta=30^0$ and equal to 0.7 times the slot width. For all the cases H/b=4 shows the maximum Nusselt number.

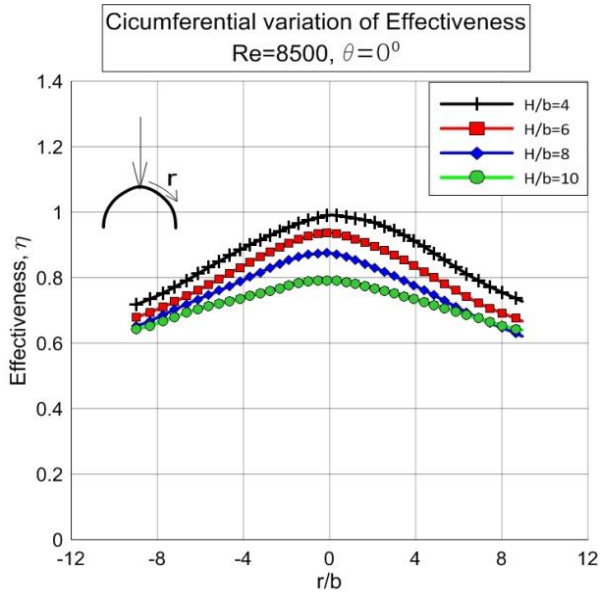

Fig. 7 Circumferential variation of Effectiveness for $\theta=0^0$ and Re=8500

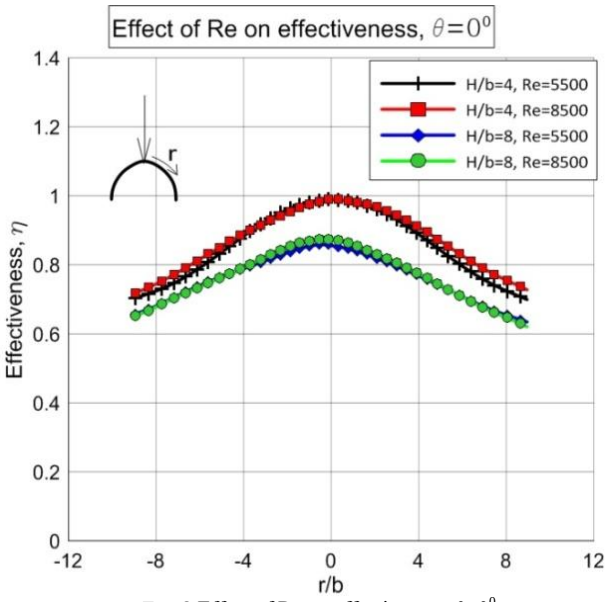

Fig. 8 Effect of Re on effectiveness, $\theta=0^0$

Along the increasing circumferential direction from the peak value zone, Nu decreases as inclination increases both on uphill and downhill sides due to the thickening of the boundary layer. The boundary layer thickens more rapidly due to the adverse pressure gradient on the uphill side resulting in a steeper drop of the Nusselt number values after the peak when compared to the downhill side. The drop is noticed to be higher for the higher inclination angle. As H/b increases maximum Nu values for inclined jets decrease and come below straight jet values since the stagnation zone is much larger due to which the jet momentum is smaller compared to the normal impingement case. However, while the trend with varying H/b is clearly visible, the differences in magnitude of the Nusselt number are within the calculated uncertainty limits.

ISBN: 978-988-14047-0-1
ISSN: 2078-0958 (Print); ISSN: 2078-0966 (Online)

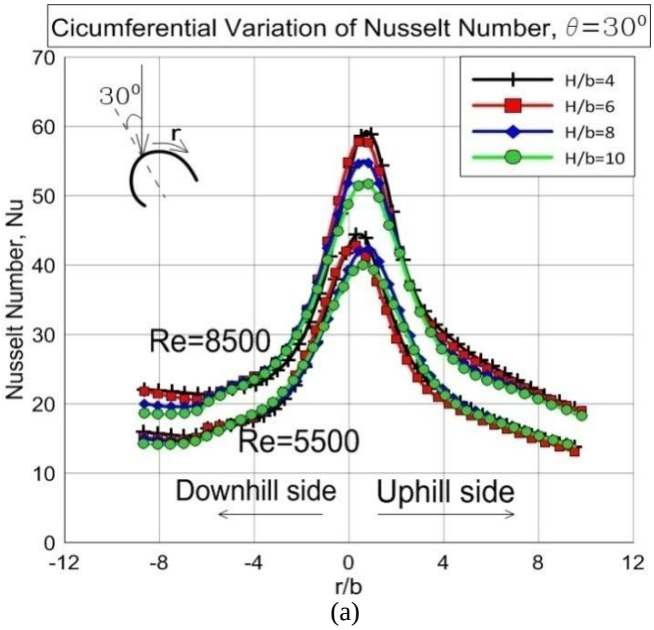

Fig. 9 Circumferential variation of Nusselt number for inclined jet (a) θ=30⁰ (b)θ=45⁰

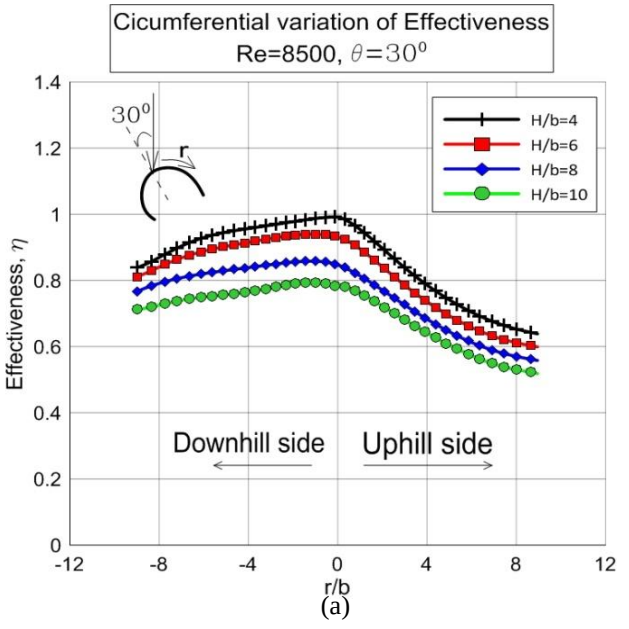

Fig. 10 Circumferential variation of effectiveness for inclined jet for Re=8500 (a) θ=30⁰ (b)θ=45⁰

Fig. 10 shows the variation of effectiveness for θ=30⁰ and 45⁰ for Re= 8500. The influence of inclination angle can be seen to be quite more prominent for the effectiveness results when compared to the Nusselt number results. The variation of effectiveness on downhill side is less, and the high effectiveness values persist to longer lengths downstream of the stagnation point. The region where the effectiveness is high on the downhill side increases with increase in inclination angle. This behavior is observed for all the jet to impingement plate distances reported in this study. The flow accelerates on the downhill side due to which entrainment is smaller which results in higher effectiveness values. The flow decelerates on the uphill side and the rapidly growing boundary layer entrains larger quantities of surrounding air resulting in reduced effectiveness values.

Fig. 11 shows effect of Reynolds number on effectiveness for both inclinations. It is observed that effect of Reynolds number is negligible in inclined impingement case also.

Fig. 12 shows variation of stagnation point Nu and maximum Nu for the different jet-to-plate distances studied. For θ=0⁰, stagnation Nu increases with H/b till H/b=6 and 8 for Re=5500 and 8500 respectively, after which the value drops. For inclined jets, both stagnation and maximum Nu decreases with H/b. The increased Nusselt number values for the normal injection with increase in H/b from very low values is typically due to a combination of the shear layer turbulence propagating inwards to the potential core and the impinging jet momentum. For an inclined jet since a larger area of the surface is exposed to shear layer turbulence the peak values of Nusselt numbers are experienced at the smallest H/b values. The subsequent fall in Nusselt numbers at higher H/b values is due to reduction in the jet momentum.

ISBN: 978-988-14047-0-1
ISSN: 2078-0958 (Print); ISSN: 2078-0966 (Online)

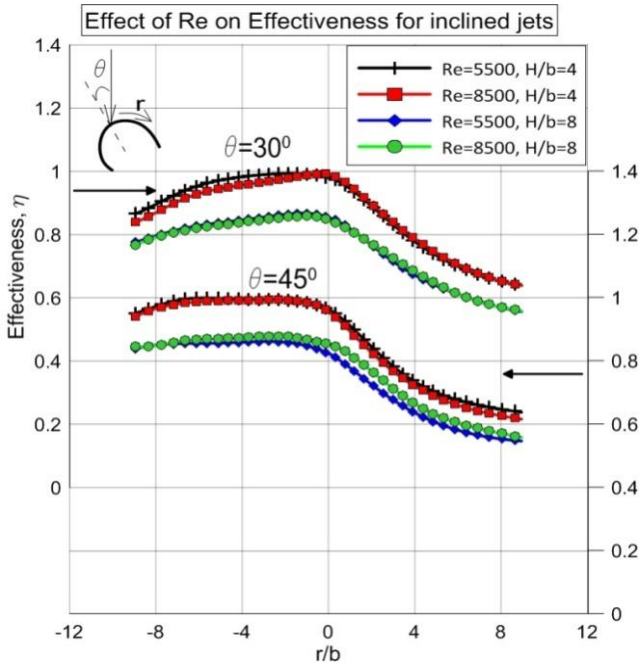

Fig. 11 Effect of Re on effectiveness for inclined jet

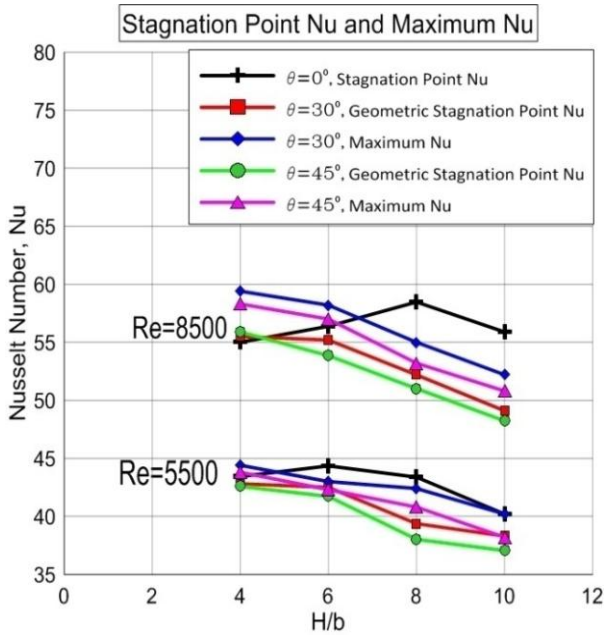

Fig. 12 Stagnation Points and Maximum Nusselt Number variation with H/b

Fig. 13 shows variation of effectiveness with H/b for all inclinations and Reynolds numbers. Effectiveness reduces continuously as H/b increases because of increased entrainment as jet to plate distance increases. Effect of inclination on stagnation point effectiveness is negligible at any given particular value of H/b.

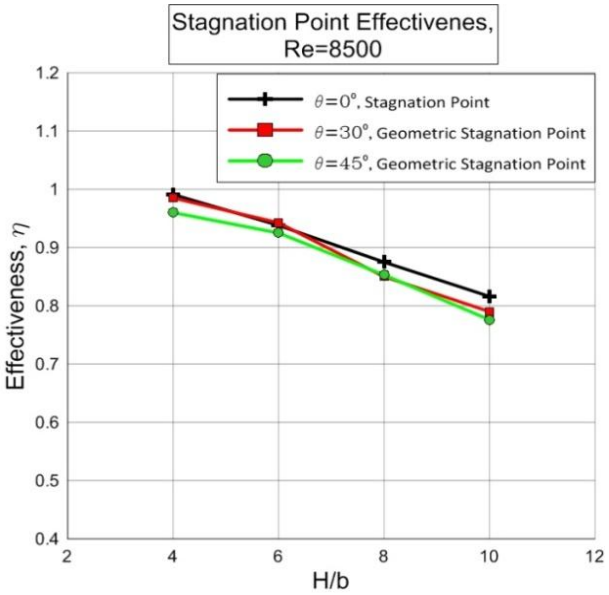

Fig. 13 Variation of effectiveness with H/b for Re=8500

IV. CONCLUSIONS

An experimental investigation for impingement of a slot jet on a cylindrical convex surface has been reported here. The presence of obliquely impinging jets causes a shift in the maximum Nusselt number towards the uphill side. The highest Nusselt number values are observed at the closest jet to surface spacing for all inclination angles in contrast to the normal impingement case where the Nu first rises and then falls.

The inclination affects the effectiveness significantly with higher values observed in the downhill region. The zone where the effectiveness is high on the downhill side increases with increase in inclination angle. This behavior is observed for all the jet to impingement plate distances reported in this study. The effectiveness values reduce on the uphill side with increase in inclination angle.

REFERENCES

[1] C. Gau, C. M. Chung, "Surface Curvature Effect on Slot-Air-Jet Impingement Cooling Flow and Heat Transfer Process", *J Heat Transfer*, vol. 113, pp. 858-864, 1991

[2] D. H. Lee, Y. S. Chung, D. S. Kim, "Turbulent flow and heat transfer measurements on a curved surface with a fully developed round impinging jet", *Int. J. Heat Fluid Flow*, Vol. 18, pp. 160-169, 1997

[3] K. B. Lim, C. H. Lee, N. W. Sung, S. H. Lee, "An experimental study on the characteristics of heat transfer on the turbulent round impingement jet according to the inclined angle of convex surface using the liquid crystal transient method", *Exp. Therm Fluid Sci.*, vol. 31, pp. 711-719, 2007

[4] R. J. Goldstein, K. A. Sobolik, W. S. Seol, "Effect Of Entrainment On The Heat Transfer To A Heated Circular Air Jet Impinging On A Flat Surface ", *J Heat Transfer*, vol. 112, pp. 608-611, 1990

[5] B. R. Hollworth, S. I. Wilson, " Entrainment Effects on Impingement Heat Transfer: Part I-Measurements of Heated Jet Velocity and Temperature Distributions and Recovery Temperatures On Target Surface**",** *J Heat Transfer*, vol. 106, pp. 797-803, 1984

[6] D. T. Vader, F. P. Incropera, R. Viskanta, "A Method for Measuring Steady Local Heat Transfer to an Impinging Liquid Jet **",** *Exp. Therm Fluid Sci.*, vol. 4, pp. 1-11, 1991

[7] M. Fenot, J.J Vullierme, E. Dorignac, "A heat transfer measurement of jet impingement with high injection temperature", *C. R. Mecanique*, vol. 333, pp. 778-782, Oct 2005.

[8] H. W. Coleman, W. G. Steele,Jr., "*Experimentation and Uncertainty Analysis For Engineers*", New York : John Wiley, 1989, ch. 3.

ISBN: 978-988-14047-0-1
ISSN: 2078-0958 (Print); ISSN: 2078-0966 (Online)